Available online at www.sciencedirect.com
SCIENCE DIRECT®
Journal of Power Sources 144 (2005) 313–321
JOURNAL OF POWER SOURCES
www.elsevier.com/locate/jpowsour

Saturation influences on the performance of valve-regulated lead–acid batteries

Barry Culpin[a,*], Ken Peters[b]

[a] *11 Bluebell Close, Whittle-le-Woods, Chorley PR6 7RH, UK*
[b] *Battery Design and Manufacturing Systems, Glenbank, 77 Chatsworth Road, Worsley, Manchester M28 2GG, UK*

Received 10 June 2004; accepted 11 October 2004
Available online 8 December 2004

Abstract

Examples of the effect of changes in separator saturation on the discharge performance and recharge effectiveness of valve-regulated lead–acid cells are given. Low-rate discharge performance decreases linearly with saturation. With the change in conductivity being distinctly non-linear, however, the high-rate capacity decreases substantially at low saturation. Cells become increasingly difficult to recharge effectively below critical saturation levels. These changes are influenced by the distribution of electrolyte within the separator. Using a simple model, the influence of the separator structure is examined. Low-rate capacity is independent of separator structure, consistent with it being able to wick electrolyte to the full height of the cell without significant variation of saturation. The preferred structure for a stable high-rate performance is low tortuosity, high anisotropy, and a low bulk density. Conversely, the recharge efficiency is best maintained as cells dry out with a structure having high tortuosity, minimum anisotropy, and small and uniform pore size. It is concluded that fibrous separators of this type should be designed according to the requirements of the application.
© 2004 Elsevier B.V. All rights reserved.

Keywords: Capacity; Recharge efficiency; Separator saturation; Valve-regulated lead–acid battery; Tortuosity; Anisotropy

1. Introduction

Over 90% of standby batteries used to provide secure, reliable telecommunications and emergency services are valve-regulated lead–acid designs. These batteries are often based in office environments or in inaccessible locations where their specific operational characteristics are beneficial. Premature failure in early designs was not uncommon, but it is now widely accepted that valve-regulated lead–acid (VRLA) batteries made by major manufacturers and operated according to specific recommendations meet service requirements. There is still concern, however, over their reliability in applications that require deep cycling. Accordingly, they are not widely used for these duties even though they offer high power capability, improved packaging flexibility, zero maintenance, and the convenience of safe location.

A key component of VRLA batteries is the separator. Whilst separators in flooded cells have a simple but important function, namely, to allow maximum possible ionic conductivity and zero electronic conductivity, separators in VRLA batteries must also provide pathways for the transport of gas to achieve the necessary level of oxygen recombination. This dual requirement, i.e., ensuring good ionic transport whilst maintaining a structure that allows gaseous diffusion, brings battery-related properties into conflict as will be shown in this paper.

An important design feature of VRLA batteries is the volume of electrolyte in each cell in relation to the amount of separator. Manufacturing methods vary but the required electrolyte volume is achieved either by careful filling, often under vacuum, or by adding excess acid, again under vacuum, and gassing off by controlled overcharge to the desired satura-

* Corresponding author. Tel.: +44 1257 270439.
E-mail address: bculpin@beeb.net (B. Culpin).

0378-7753/$ – see front matter © 2004 Elsevier B.V. All rights reserved.
doi:10.1016/j.jpowsour.2004.10.013

tion level. The evacuation process ensures that the electrolyte is uniformly dispersed in both the porous plates and separators. With the active materials having appreciably smaller pores than the fibrous separator, they fill first and retain acid in preference to the separator. Consequently, the term 'saturation' in this study refers to the extent to which the pores in the separator are filled and is defined as the percentage of the pore volume in the separator that is filled with acid.

Whilst VRLA batteries are designed and made with a specific saturation, the oxygen recombination cycle is never 100% efficient and, consequently, some water is lost during charge. Also, chemical and structural changes of the active materials during cycling result in some re-distribution of the electrolyte. Changes in the saturation level can have a significant influence on both the discharge performance and the recharge characteristics, as will be shown. The aim of this study is to review the effect on battery-related properties and by using a simple model to consider how the structure of the separator may influence these properties.

2. Separator structure

Excepting gelled designs, which are not considered in this study, separators in VRLA batteries consist of microfibres of borosilicate glass made by wet laying in conventional papermaking style. This material has a high chemical resistance and good wetting characteristics, and separators can be made with a high pore volume and small pore size. The wet-laying process produces an anisotropic structure with different tensile properties and pore-size distribution across the three dimensions. Pore size measurements that are commonly carried out do not fully represent the complex network of fibres.

Glass fibres used in making absorbent glass mat separators have diameters that range from 0.25 to 4 μm with a typical length of 1 mm. Details of how the fibre length and surface area change with diameter are given in Table 1. Although fibres are randomly orientated, they lie predominantly in the plane of the sheet with the largest pores in the *z* (thickness) dimension.

A simple and effective model of a VRLA separator can be achieved by considering it to be composed of cubic pores of equal size, with the sides defined by the glass fibres. For the purpose of this model, the separator is considered to have a thickness of 1 mm and a bulk density of 150 g m^{-2} mm^{-1} of thickness. The density of the glass is assumed to be 2360 kg m^{-3}. Applying this model to the question of pore anisotropy gives a linear relationship between fibre diameter and pore size, as shown in Fig. 1. In comparison, experimental results from previous work [1] shows pores in the *x* and *y* dimensions, determined by measuring the wicking rate and applying the Washburn equation, are smaller than predicted by the model whilst pores in the *z* dimension (thickness), determined by the maximum bubble technique, are larger than predicted. Both sets of experimental data show the same linear relationship between pore size and fibre diameter. This finding is expected from the anisotropy of the separator. The pore size predicted by the model lies between the two sets of experimental data (the model assumes uniform pore size) and gives credence to this approach.

Table 2
Saturation influences on performance

Saturation (%)	Reserve capacity (min)	30-s volts at 625 A/−18 °C
95	88	8.0
89	84	7.9
83	80	7.6
75	74	7.0
68	70	6.1

3. Effect of saturation on battery behaviour

3.1. Discharge performance

Several authors have shown [2,3] the effect of electrolyte volume on capacity in limited electrolyte designs of lead–acid cells. As an example, the results of trials on valve-regulated designs of automotive batteries consisting of 11 plates per cell with a nominal cold-cranking current of 625 A at −18 °C and a reserve capacity of 85 min at 25 A (25 °C) when filled with different amounts of electrolyte are given in Table 2. Uniform dispersion of the electrolyte was assured by the application of several vacuum pulses. The saturation of the separator was between 95% and 68%.

The change in the reserve capacity follows a linear relationship, proportional to the saturation (Fig. 2), as does the capacity at similar low rates of discharge, not reported here. Both the resistivity and the 30-s voltage at different saturations are shown in Fig. 3. The data demonstrate the effect on high-rate performance due to the increasing resistance as saturation decreases, as previously reported [4].

Table 1
Effect of diameter on surface area and length of glass fibres

Diameter (μm)	0.1	0.5	1.0	2.0	5.0
Length (m kg^{-1})	4.7×10^{10}	1.9×10^{9}	4.7×10^{8}	1.2×10^{8}	1.9×10^{7}
Length (m m^{-3})	1.1×10^{14}	4.5×10^{12}	1.1×10^{12}	2.8×10^{11}	4.5×10^{10}
Surface area (m^2 kg^{-1})	14800	2960	1480	741	296
Surface area (m^2 m^{-3})	3.5×10^{6}	7.1×10^{5}	3.5×10^{5}	1.8×10^{5}	7.1×10^{4}

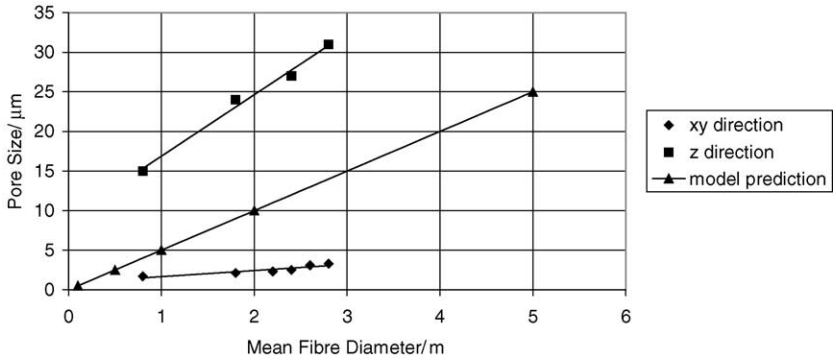

Fig. 1. Effect of fibre diameter on pore size: comparison of experimental measurements in *x*, *y* and *z* dimensions and model prediction.

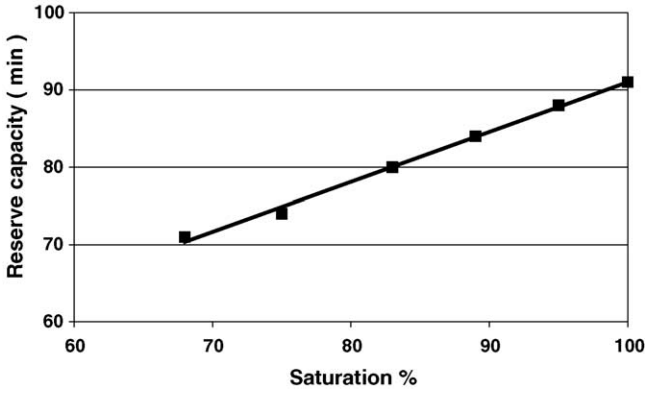

Fig. 2. Effect of saturation on reserve capacity.

3.2. Recharge influences

Conventional practice is to recharge cells or batteries to a pre-determined voltage that is indicative of a satisfactory state-of-charge of both the positive and negative plates. With valve-regulated designs, this can be misleading since at high levels of gas recombination the negative plate may be depolarized by the oxygen reduction reaction and its potential may remain close to its equilibrium potential. Without limiting control of current or time, cells will be overcharged and in extreme conditions temperatures may rise with the risk of a thermal runaway cycle with the cell voltage further decreasing as current and temperature continue to rise.

The above effects are influenced by the oxygen transport through the separator, the rate of which is critically dependent on the saturation of the separator. Measurements of oxygen diffusion through separators have shown that at low saturation (<60%), diffusion rates similar to gaseous diffusion are possible, whilst at high saturation (>90%) the rates are several orders of magnitude lower and are similar to those through a liquid [4], as illustrated in Fig. 4. The diffusion rates at high saturation will only support efficient recombination at low charging currents such as in standby service where, under float conditions, oxygen-recombination efficiencies approaching 100% are possible. Under these conditions, gas transport occurs by oxygen creating a differential pressure across the separator, which displaces electrolyte from larger pores, and passing through the separator in preference to moving into the headspace. At higher currents, water is lost and the saturation decreases to a point where the oxygen transport mechanism changes from a pressure-assisted mechanism to free diffusion. At this point, the diffusion rate increases exponentially and supports the oxygen cycle at higher currents.

The influence of unrestricted oxygen transport on charge patterns is best illustrated by comparing the Tafel slopes for cells with flooded or limited electrolyte (Fig. 5). In flooded cells with zero recombination, the sum of the two Tafel slopes is 210 mV per decade compared with 90 mV per decade in a

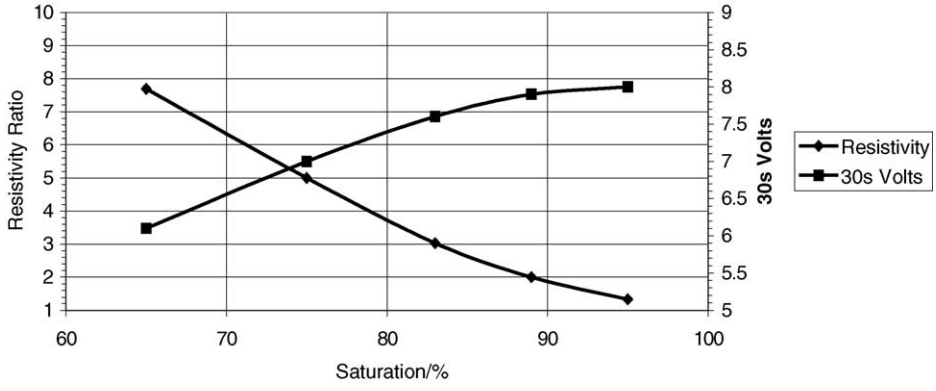

Fig. 3. Change in 30-s voltage and cell resistivity with saturation.

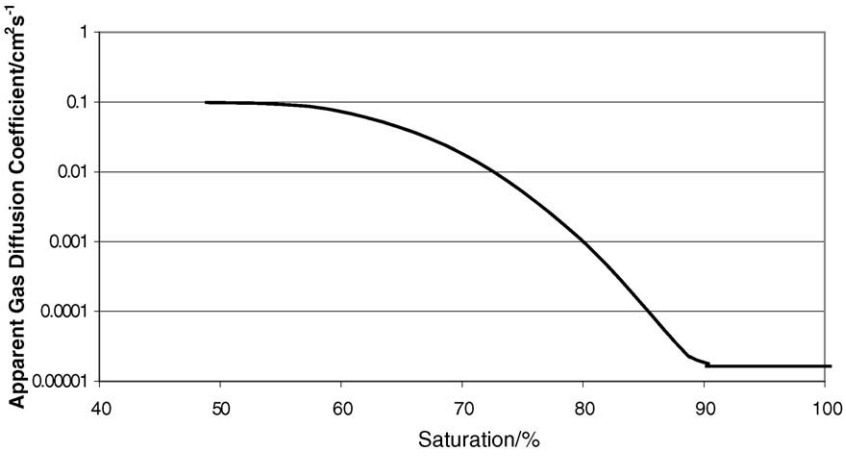

Fig. 4. Effect of separator saturation on oxygen diffusion [4].

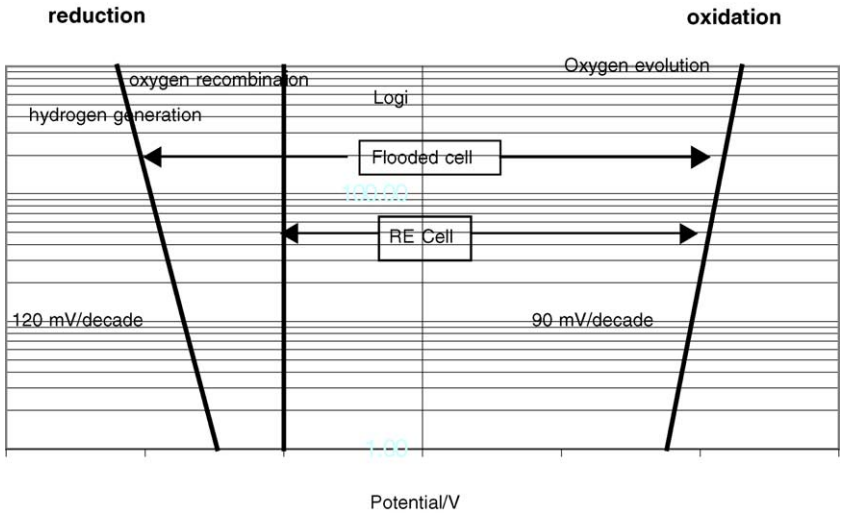

Fig. 5. Tafel slopes in flooded and recombination environments.

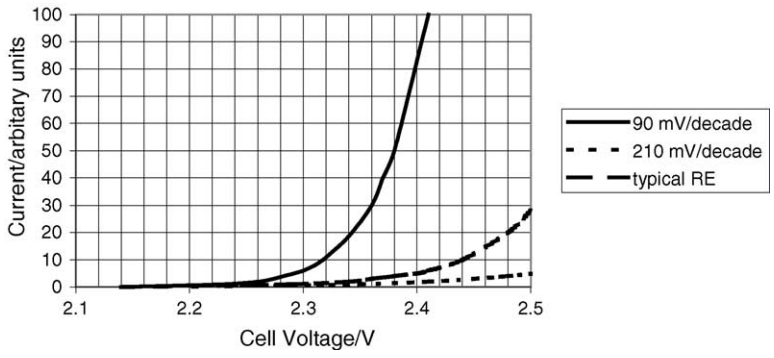

Fig. 6. Effect of voltage on overcharge current for RE and flooded systems.

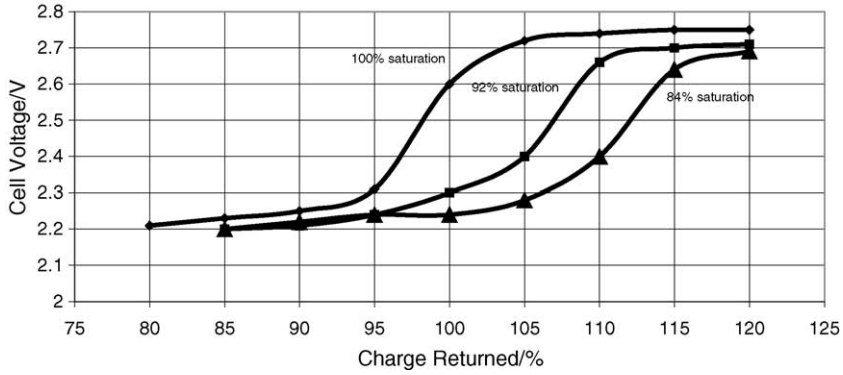

Fig. 7. Effect of saturation on recharge efficiency characteristics of tubular cells [6].

recombinant design that operates with 100% recombination efficiency.

The practical significance of this is shown by comparing the influence on charging under constant-potential conditions (Fig. 6). In recombinant designs with unrestricted gas transport through the separator, the charge current is five times that of flooded cells at 2.25 V and 25 times greater when floated at 2.35 V, most of which supports the oxygen reduction reaction. (Note: the open-circuit voltage of the cells is 2.14 V.)

Included in Fig. 6 is a third line that represents a typical recombination-electrolyte (RE) cell recombining at 97% at a voltage of 2.28 V, which uses data taken from a recent study on the thermal runaway in VRLA cells [5]. This cell shows appreciably lower currents at specific voltages than cells that exhibit 100% recombination.

Comparable effects with valve-regulated designs of tubular cells made with varying amounts of electrolyte have been reported by Dyson and Griffin [6]. Polarization to gassing voltages is increasingly delayed with increasing under-saturation, as shown in Fig. 7. When fully saturated, the voltage increases towards the gassing potential after a charge input of approximately 98% and the charge input is voltage limited before the cell is fully charged. At low saturation (∼84%), the voltage-limited overcharge at approximately 10% of capacity is unnecessarily high.

4. Discussion

A decrease in saturation affects both the discharge and recharge behaviour of valve-regulated cells. When the saturation is high, efficient oxygen recombination is only possible at low overcharge currents and under such conditions there is little water loss. If overcharge currents are high, gas-transport constraints result in water loss until sufficient oxygen transport is possible and, consequently, the discharge capacity decreases and the internal resistance increases. At

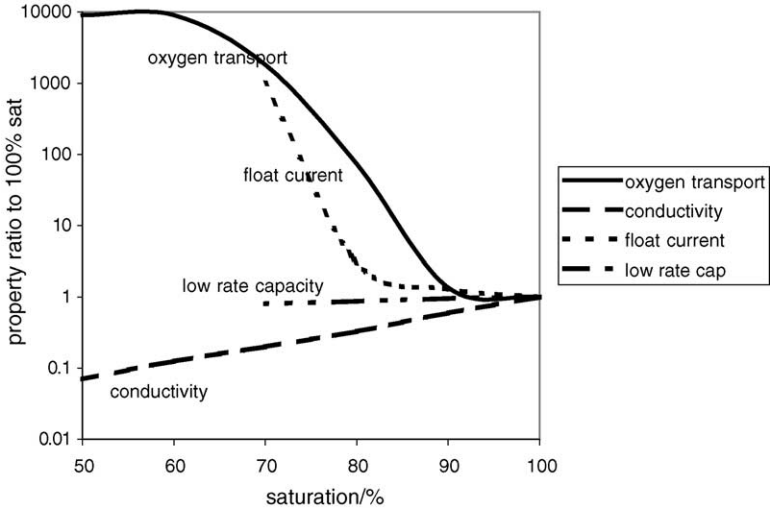

Fig. 8. Summary of saturation effects. Note: Properties are related to a nominal value of 1 at 100% saturation and are designed to show the extent of the changes and have no units. The *Y*-axis is a log scale.

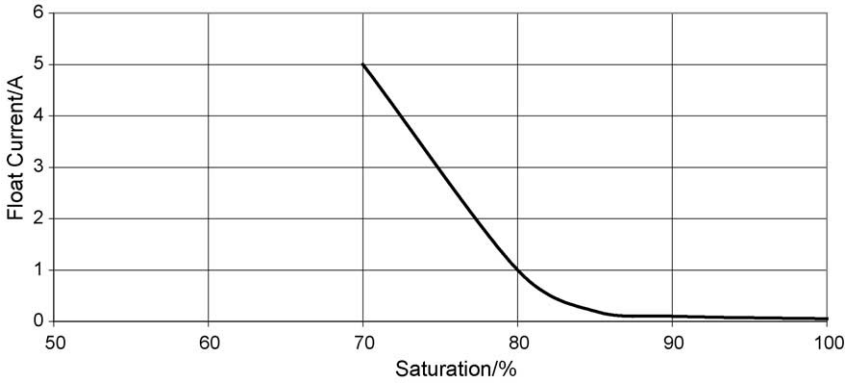

Fig. 9. Effect of separator saturation on float current at 2.28 V_{pc}.

low saturation, the high diffusion rate of oxygen makes it increasingly difficult to charge the negative plate efficiently. These changes are summarized in Fig. 8.

The distribution of electrolyte in the separator depends on its structure. Due to the high air|liquid interfacial tension, the area of contact with the glass fibres is maximized with minimum surface in contact with the gaseous phase. Small pores fill first and leave larger pores open, free to the passage of gas. As filling proceeds, pores of increasing size are blocked. At around 90% saturation, larger pores are bridged and the residual 10% by volume of gas is contained within isolated and discontinuous bubbles that play no effective part in gas transport. Pores empty in the reverse order, i.e., largest first, as water is lost during service.

Experience shows that oxygen recombination is possible when the saturation is reduced to approximately 98%. As described in Section 3.2, at this saturation level the passage of oxygen through the separator is by a pressure-assisted mechanism and at low charge currents recombination efficiencies of the order of 95–97% are possible. With further loss of water, continuous pathways are created. This changes the oxygen-transport mechanism to diffusion and high recombination efficiencies are possible, even at high currents. Oxygen reduction becomes the main electrochemical reaction at the negative electrode with the possibility that the negative electrode is not polarized but remains close to its equilibrium potential. The potential of the positive electrode shifts to a more positive value and without current limitation, a runaway situation may develop. Progressive sulfation of the negative plate is likely on repetitive cycling.

The implication of the above behaviour is that there is a critical saturation at which point the mechanism of gas transport changes and beyond which effective recharge becomes increasingly difficult. The concept of a critical saturation point is supported by results from a previous study [6] that showed the current response at 2.28 V per cell to increase at an uncontrolled rate at saturations below 85%, as illustrated in Fig. 9. It follows the same pattern as the change in gas-diffusion rate given in Fig. 4.

Although the recharge response remains relatively stable until the critical saturation point, the discharge capacity decreases progressively as water is lost, most noticeably at high rates, due to the significant decrease in conductivity across the separator. Conductivity measurements have demonstrated that the change with saturation is distinctly non-linear; it decreases by 50% when the saturation reduces from 97% to 85%. This is surprising since with a pore tortuosity that approximates unity and a high pore volume, the conductivity of a saturated separator should approach that of bulk sulfuric acid and decrease linearly according to the amount of

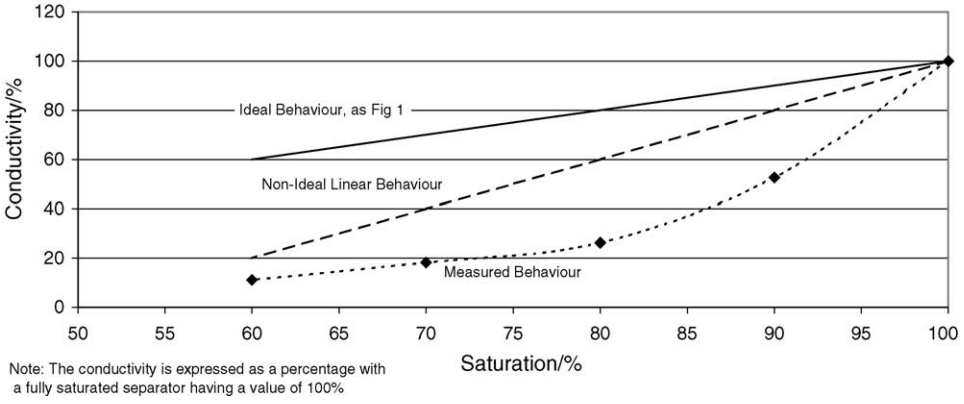

Fig. 10. Comparison of the measured change in conductivity as saturation decreases with the ideal situation.

retained electrolyte. The difference is presented in Fig. 10 where experimental data is compared with a linear ideal relationship that is based solely on the uniform loss of water from the pores. As discussed later, water loss will most likely create gas channels of a meandering nature and the conductivity will decrease in a non-ideal linear way, as also shown in Fig. 10. In a partially saturated porous media, the extent of these effects, namely the variation in conductivity from the ideal behaviour and the effect on recharge as saturation changes, are influenced by the structure of the separator, as will now be considered.

4.1. Effect of separator structure

The anisotropic structure of glass microfibre separators provides the necessary characteristics to support the essential operational features of valve-regulated batteries. Small pores in the *x* and *y* dimensions distribute electrolyte and maintain wicking when partially saturated. Meanwhile, the larger pores in the *z* dimension assist gas transport with gas moving preferentially through the *z* plane to the negative plate rather than up or across the *x* and *y* planes. When recombination is inadequate, the saturation decreases through the preferential removal of water in the *z* plane.

As discussed previously, oxygen transport through the separator at high saturation levels is pressure-assisted with the relationship between pore diameter and the pressure to move electrolyte defined by the Laplace equation:

$$P = 2\gamma\left(\frac{1}{r_2} - \frac{1}{r_1}\right)$$

where P is the pressure required to move electrolyte from a pore of radius r_1 to a pore of radius r_2 and γ the surface tension of the electrolyte.

The relationship between pressure and size of pore is given in Fig. 1. The pressure required to move electrolyte from 20 to 30 μm, which are typical *z* plane dimensions, is approximately 0.5 kN m^{-2}, whilst pressures in excess of 50 kN m^{-2} are required to force electrolyte from 2 to 4 μm pores that are in the *x* and *y* planes (Fig. 11).

As shown in Fig. 1, decreasing fibre diameter reduces pore diameters in both planes linearly, but the change is greater in the *z* plane than in the *x* and *y* planes. Separators made with fibres of small diameter (∼1 μm) will have improved wicking whilst gas transport will be more difficult than through separators composed of fibres with larger diameter.

For a model of a network of cubic-shaped pores (described in Section 2), the random distribution of fibres with a 2 μm diameter gives a structure with a pore size of 10 μm. The model assumes uniform pores of the same size that empty at random with no preference for those that empty first. It is suggested that the critical change from pressure-assisted transport to pure diffusion will be at a lower saturation level in such a structure or one in which the pores across the three dimensions are more uniform.

In a three-dimensional structure of pores of uniform size, percolation theory predicts that the transition to continuous open pathways starts at about 60% saturation. It is interesting to note recent measurements of diffusion rates through a different separator have given a similar transition point [7] whereas the results in Fig. 8 show the change in oxygen transport occurs at a saturation of about 85%. Delays in this transition point would result in characteristics closer to the ideal situation described earlier, with high recharge efficiency being maintained over a wider saturation range.

As described earlier, the wet-laying process of glass fibres produces a complex network of fibres lying predominantly in the plane of the sheet. Three conceptual fibre distributions are illustrated in Fig. 12. Pores aligned perpendicular to the electrode surface provide optimum conductivity for a given saturation (Fig. 12(a)). Ions travel the shortest distance between electrodes i.e., the tortuosity is at a minimum with a linear relationship between saturation and conductivity. The gas and liquid channels in Fig. 12(b) remain essentially perpendicular to the plate surfaces but meander to a degree through the separator. The ionic pathway is extended and hence the conductivity is lower than in Fig. 12(a) at an identical saturation. The more the convolution, the greater is the effect of saturation on conductivity. The third diagram, Fig. 12(c), is an extreme example and unlikely to occur in practice as gas channels necessary for gas transport do not connect the elec-

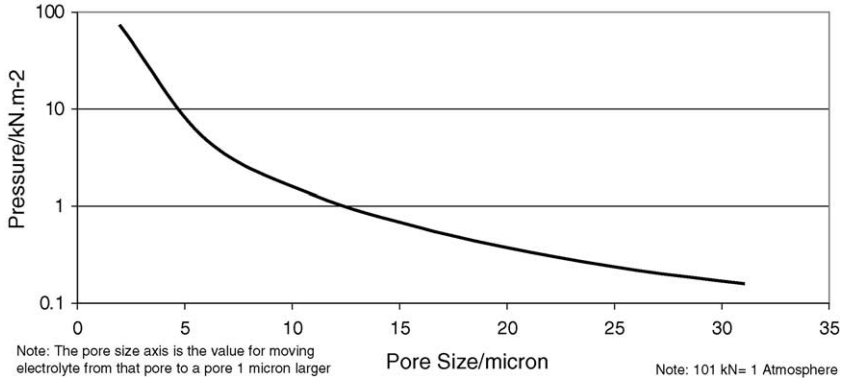

Fig. 11. Pressure required to move electrolyte between pores of different sizes.

trodes at the top and bottom of the diagram. It is included as a situation in which ionic transport is severely hindered with a tortuous route from the top to the bottom of the diagram.

In the first example, as water is lost from the separator the conductivity/saturation relationship will follow the ideal linear relationship shown in Fig. 10. Loss of water from the more realistic situation in Fig. 12(b) provides several possibilities. More gas channels of an equal meandering nature are created and the conductivity will decrease linearly as the saturation decreases. This is shown as non-ideal linear behaviour in Fig. 10. A second possibility is that the degree of meander changes and it may be easier or more difficult for gas to find the large, easily emptied pores as the separator loses electrolyte. In these circumstances, the relationship between saturation and conductivity becomes non-linear. A further possibility is that gas pathways become branched and thereby isolate pockets of electrolyte in 'dead-end pores'. Whilst it is assumed all gas channels are connected and extend from one side of the separator to the other, some gas pockets could exist in isolation and in these instances the relationship between saturation and conductivity becomes non-linear and approaches that of the experimental data.

The increased tortuosity that results from the unlikely structure in Fig. 12(c) is self-explanatory. This structure may also include pores that are isolated in the centre of the separator that do not contribute to the gas flow but contribute to the tortuosity and hence reduce the conductivity. A measure of the lack of understanding of this system is that there is no indication of how much closed porosity exists in partially saturated separators.

4.2. Application considerations

The above review suggests that there is considerable conflict between the structure and the characteristics of those fibrous separators that are most suitable for both stable conductivity and gas-diffusion characteristics over a wide range of saturation. It is therefore difficult to satisfy both requirements. For example, applications that require minimal change in resistance and power as saturation decreases

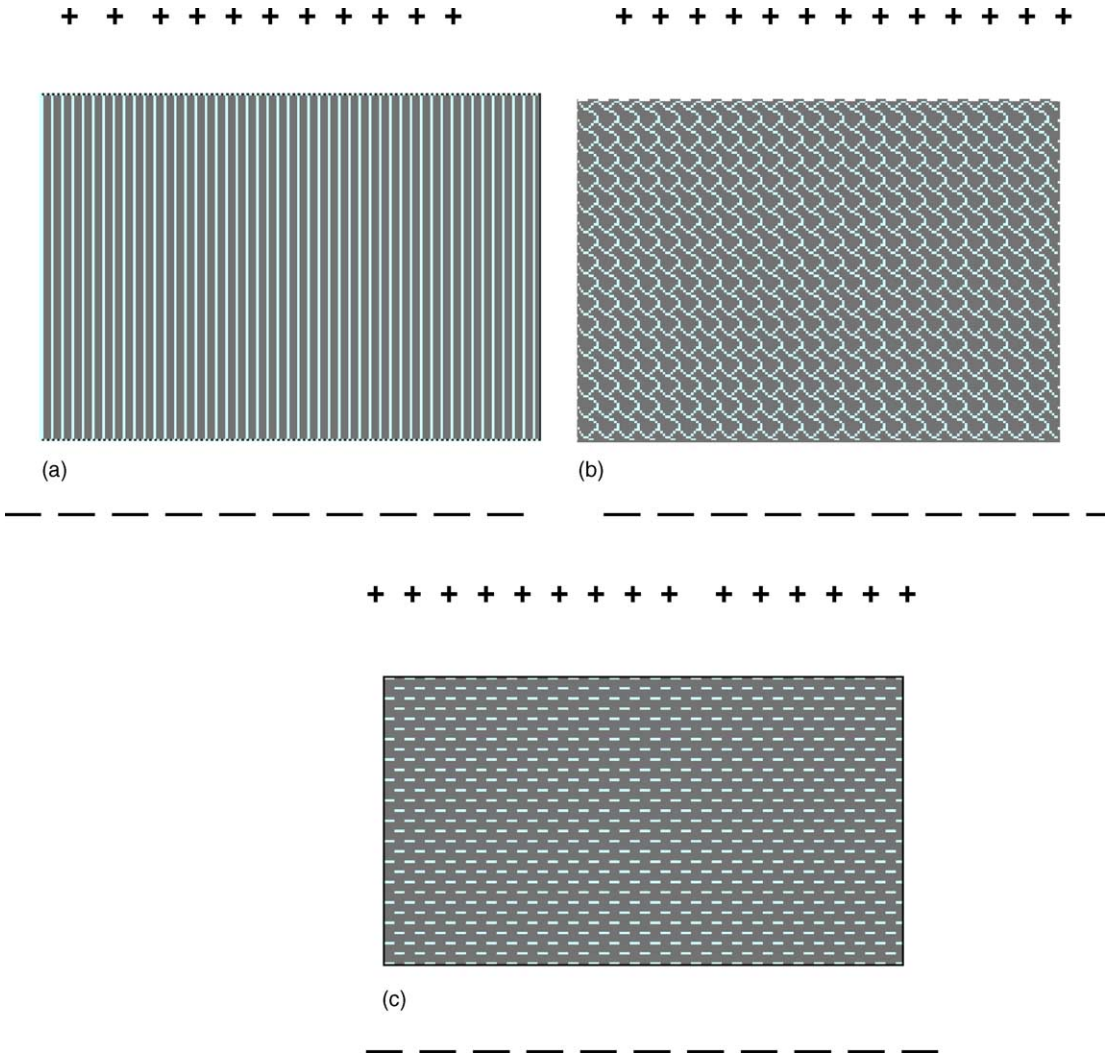

Fig. 12. (a) Idealized parallel-sided, (b) meandering gas pores, (c) gas channels parallel to electrode surface.

Table 3
Structural preferences for glass-fire separators in VRLA batteries

Property	High-rate performance	Low-rate performance	Recharge efficiency
Anisotropy	High	No effect	Low
Tortuosity	Low	No effect	High
Pore size	Large	No effect	Small
Pore-size distribution	No effect	No effect	Low

are best satisfied using separators with large pores that extend linearly in the *z* plane. Ideally, the pores should have a uniform size, or more practically a small size distribution with a minimum number of fibres crossing the pores. A low bulk density is preferable. Such structures can be achieved by ensuring that a maximum number of fibres lie in the plane of the paper (*x* and *y* dimensions) so as to reduce the tortuosity in the *z* plane and maximize the anisotropy of the structure. The low-rate capacity is a linear function of the separator saturation, i.e., it is directly proportional to the amount of acid present. It is unlikely that any change to the structure of the separator will affect this relationship.

Conversely, maintenance of recharge efficiency as the separator dries out, i.e. by ensuring the transport of oxygen proceeds via a pressure-assisted diffusion mechanism at as low a saturation level as possible, is best achieved with a structure containing pores of equal size so that they empty at random and provide maximum dry-out before open gas pathways are formed. The method of separator manufacture precludes this ideal situation but helpful factors are reduced anisotropy (making pore sizes in the *z* dimension close to those in the *x* and *y* planes), small pore size (increasing the number of pores per unit thickness of separator), and a low pore-size distribution.

In practical terms, valve-regulated batteries in standby applications require operational stability and stable recharge efficiency as water is lost rather than high power capability, whereas automotive batteries require high starting power throughout service. Clearly, the separator requirements to best meet these operational demands are in conflict and suggest that separators should be designed specifically for a given application.

In some duties, however, it is essential to maintain recharge efficiency and a high power capability. For example, the new generation of VRLA batteries used as auxiliary power sources in hybrid powered vehicles must provide and absorb relatively high current pulses over a long calendar life whilst operating in a partial state-of-charge condition. Experience to date shows early capacity decline due to negative sulfation. Whilst several design and operational factors may contribute to this degradation in performance, the significant change would appear to be a decrease in saturation to a critical level beyond which effective recharge becomes increasingly difficult.

5. Conclusions

Efficient oxygen recombination in highly saturated VRLA cells is only possible at low overcharge currents due to the restricted passage of oxygen through the separator. With high charge currents, water is progressively lost until gas transport is sufficient to maintain efficient recombination. When this occurs, the high diffusion rate of oxygen makes it increasingly difficult to charge the negative plate efficiently.

Discharge capacities at low rates of discharge decrease linearly as water is lost. Under high-rate discharge conditions, the decrease is distinctly non-linear due to the significant decrease in conductivity across the separator.

The extent of these effects, namely the variation in conductivity and the effect on recharge as saturation changes, are influenced by the structure of the separator. Low-rate capacity is independent of the separator structure, which is consistent with it being able to wick electrolyte to the full height of the cell without significant variation of saturation throughout its height. The preferred structure for a more stable high-rate performance is low tortuosity, high anisotropy and a low bulk density. Conversely, the recharge efficiency as cells dry out is best maintained with high tortuosity and minimum anisotropy, as well as with small pore sizes with a low size distribution.

Table 3 summarises these requirements and highlights the need to design separators for the end use applications.

References

[1] B. Culpin, J. Power Sources 53 (1995) 127–135.
[2] F.J. Vaccaro, P. Casson, Proceedings of the Intelectual Conference, 1987.
[3] T.V. Nguyen, R.E. White, J. Electrochem. Soc. 137 (1990) 2998–3002.
[4] B. Culpin, J.A. Hayman, Power Sources, in: L.E. Pearce (Ed.), Proceedings of the International Power Sources Symposium Committee, vol. 11, Leatherhead, England, 1986, pp. 45–60.
[5] B. Culpin, J. Power Sources 133 (2004) 79–86.
[6] I. Dyson, P. Griffin, J. Power Sources 116 (2003) 263–282.
[7] R.J. Ball, R. Evans, R. Stevens, J. Power Sources 104 (2002) 208–220.